

Few-body decay and recombination in nuclear astrophysics

A.S. Jensen · D.V. Fedorov · R. de Diego ·
E. Garrido · R. Álvarez-Rodríguez

Received: date / Accepted: date

Abstract Three-body continuum problems are investigated for light nuclei of astrophysical relevance. We focus on three-body decays of resonances or recombination via resonances or the continuum background. The concepts of widths, decay mechanisms and dynamic evolution are discussed. We also discuss results for the triple α decay in connection with 2^+ resonances and density and temperature dependence rates of recombination into light nuclei from α -particles and neutrons.

Keywords Few-body problems · Astrophysics · Unstable nuclei

1 Introduction

Few-body problems, astrophysics and unstable nuclei are naturally linked through light nuclei being formed in few-body recombination reactions in astrophysical environments. The inverse reactions of few-body decays of light nuclei are equivalent through detailed balance. The state of the art in few-body physics is that all two-body problems and essentially all bound state three-body problems are fully solved. The next in line is three-body continuum problems where lots of information presently accumulate from kinematically complete and accurate measurements of nuclear decay processes. The simplest of these examples are nuclear three-body decays of a (many-body) resonance. A large variety of decay mechanisms is possible due to the continuous distribution of energy and momentum between the three particles in the final state. We shall here

Presented at the 21st European Conference on Few-Body Problems in Physics, Salamanca, Spain, 30 August - 3 September 2010

A.S. Jensen and D.V. Fedorov
Department of Physics and Astronomy, Aarhus University, DK-8000 Aarhus C, Denmark
Tel.: +45-8942 3655 and +45-8942 3651
E-mail: asj@phys.au.dk and fedorov@phys.au.dk

R. de Diego and E. Garrido
Instituto de Estructura de la Materia, CSIC, Serrano 123, E-28006 Madrid, Spain

R. Álvarez-Rodríguez
Departamento de Física Atómica, Molecular y Nuclear, Universidad Complutense de Madrid,
E-28040 Madrid, Spain

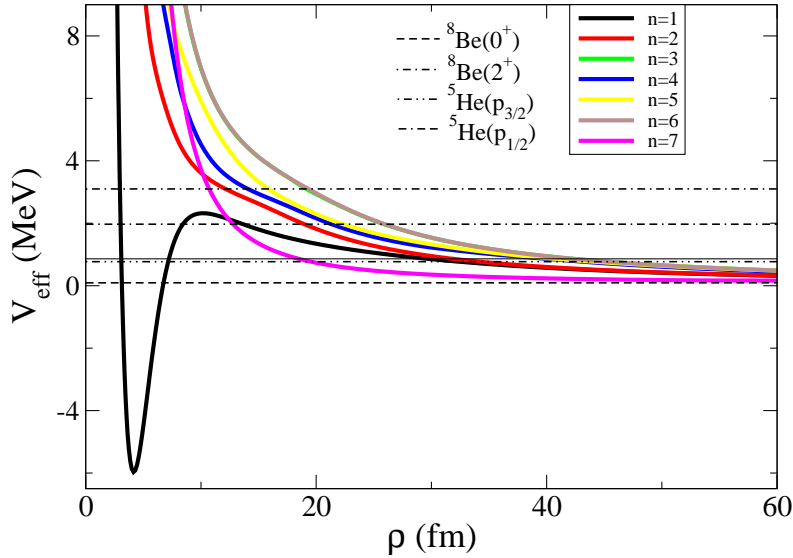


Fig. 1 The real parts for $\theta = 0.1$ of the lowest adiabatic potentials, including the three-body potential, for the 0.856 MeV ${}^9\text{Be}(5/2^-)$ -resonance (horizontal full line) as function of ρ .

focus on genuine three-body continuum computations. We shall especially emphasize the new concepts employed or discovered, and illustrate with examples of relevance in nuclear astrophysics.

2 Definitions

The minimum needed for the discussions is the hyperradius ρ defined as the mass weighted mean square radius coordinate:

$$m\rho^2 = \frac{1}{m_1 + m_2 + m_3} \sum_k m_k (\mathbf{r}_k - \mathbf{R})^2 \quad (1)$$

where m is an arbitrary mass, m_k and \mathbf{r}_k are mass and position of the k 'th particle and \mathbf{R} is the centre-of-mass coordinates. The total wave function is $\psi = \rho^{-5/2} \sum_n f_n(\rho) \phi_n(\rho, \Omega)$, where Ω denotes the five angular coordinates. The differential equations for one radial function f_n are [1]

$$\left[-\frac{d^2}{d\rho^2} + \frac{\lambda(\rho) + 15/4}{\rho^2} + Q(\rho) - \frac{2mE}{\hbar^2} \right] f_n(\rho) = \text{couplings}, \quad Q(\rho) = \langle \phi | \frac{\partial^2}{\partial \rho^2} | \phi \rangle_{\Omega}, \quad (2)$$

where E is the energy, λ is obtained from the angular equations, and Q is the non-adiabatic diagonal coupling strongly correlated to the variation of the angular wave function.

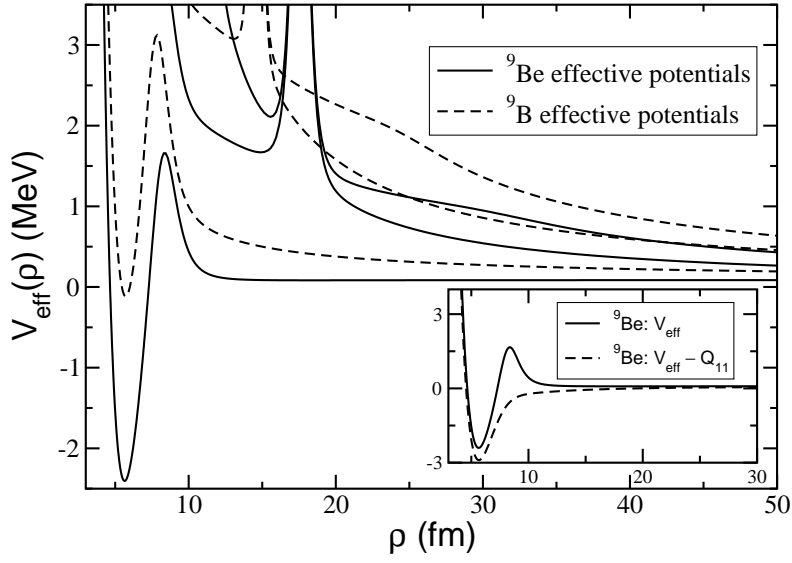


Fig. 2 Lowest adiabatic potentials for ${}^9\text{Be}$ and ${}^9\text{B}$ as a function of the hyperradius. The inset shows the ${}^9\text{Be}$ lowest potential with and without the rearrangement coupling term $Q = \langle \phi | \frac{\partial^2}{\partial \rho^2} | \phi \rangle_{\Omega}$.

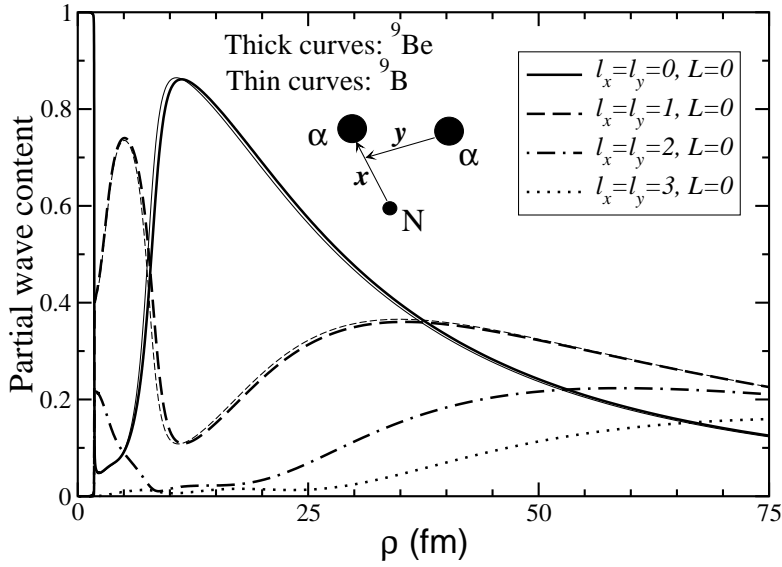


Fig. 3 The partial wave decomposition of the lowest adiabatic angular wave function for ${}^9\text{Be}$ (thick) and ${}^9\text{B}$ (thin) as function of hyperradius ρ . The partial angular momenta l_x and l_y correspond to the coordinates indicated in the figure. For $l_x = l_y = 2$ and $l_x = l_y = 3$ the curves for ${}^9\text{Be}$ and ${}^9\text{B}$ can not be distinguished.

3 Concepts in three-body decays

The key quantities are the potentials as functions of the hyperradius as shown in Fig. 1 where one potential has an attractive pocket at short distance whereas all the other potentials are repulsive. The resonance is caught in the pocket and its partial lifetime, or width, is determined by the tunneling probability through the barrier. The coordinate is ρ and *a priori* it is not clear that the width is determined by the barrier of the hyperradial potential. The angular momentum and parity dependence now follow these potentials which often lead to non-monotonous behavior. The behavior at short distances is outside the three-body model and able to influence the widths substantially in analogy to the effects of spectroscopic factors [2].

The resonance can change structure from small to large distance [3,4]. In Fig. 1 the two lowest potentials cross each other around ρ of 16 fm. The resonance then must decide whether to maintain its structure determined by the lowest potential at small distances or gain energy by changing structure. The compromise can be any continuous division between these extremes. This dynamic evolution is seen in Fig. 2 for ${}^9\text{Be}(1/2^+)$ where the inset shows that the barrier is entirely due to the Q -term in Fig. 2, see [5]. This implies that the entire width is due to angular restructuring and in fact therefore responsible for the resonance character of this state. This is demonstrated in Fig. 3 where the partial wave decomposition in one Jacobi coordinate set is shown to change drastically around ρ of 7 fm from a ${}^5\text{He}+\alpha$ to a ${}^8\text{Be}+n$ structure. This is consistent with the observation that the decay products emerge as arising fully from the latter configuration [6]. In the example of Fig. 1 this means that the lowest energy is chosen while the structure is changed at the level crossing. These examples show the concepts of dynamic evolution and decay mechanism [7].

4 Rates and momentum distributions

The inverse process of three-body decay is the recombination of the constituent clusters into the bound state of the nucleus for example by photon emission [8]. The most prominent as well as most studied of these processes is the triple α process leading to ${}^{12}\text{C}$. At low temperature the lowest 0^+ resonance, the Hoyle state, is decisive for the triple α rate which proceeds from the 0^+ continuum via an E2-transition to the 2^+ excited but bound state. The process from the 2^+ continuum is dominated by E2-transition directly to the 0^+ ground state. The position of the lowest 2^+ resonance is then important but unknown or at least controversial.

In Fig. 4 we show the results of genuine three-body computations for different positions of the lowest 2^+ resonance. The rate varies by almost two orders of magnitude when the energy is increased from 2 MeV to 5 MeV. The contribution is only significant for temperatures above 2-3 GK. The more realistic uncertainty is seen in Fig. 5 where we compare to the standard reference [9] and give the variation from the relatively small 2^+ energy of 1.38 MeV to complete removal of the 2^+ resonance. In the temperature range of around 8 GK the uncertainty in the triple α rate then comes out to be around a factor of three.

The large-distance structure of the resonance wave function provides the momentum distributions of the particles after the three-body decay [10]. The probability for emission of a particle as function of its energy is an important part of these distributions. However the complete information requires two energies for a given total

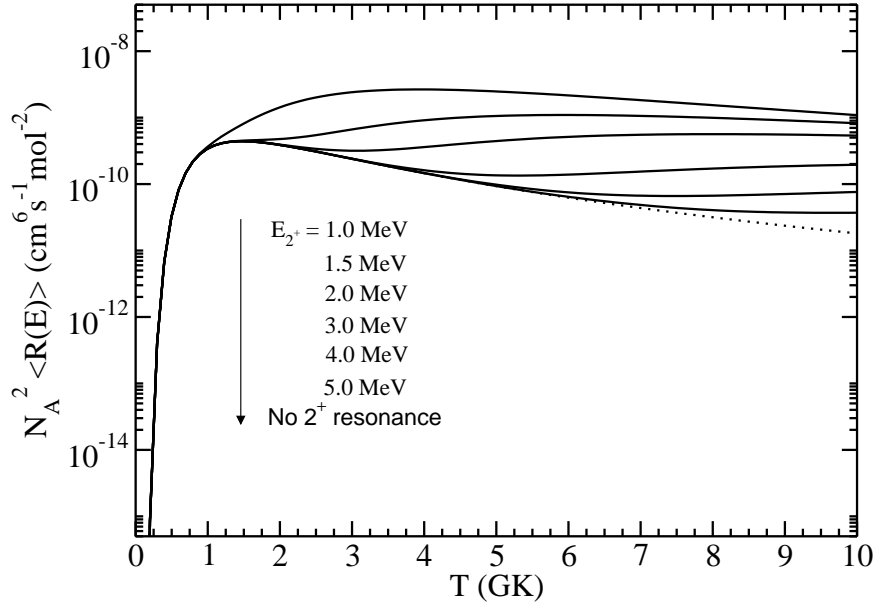


Fig. 4 Reaction rate in the sequential case for different energies of the lowest 2^+ resonance in ^{12}C . The energy increases from the upper curve to the lower from 1 MeV up to 5 MeV. The dotted curve is the calculation where the contribution from the $2^+ \rightarrow 0_1^+$ transition has been completely removed.

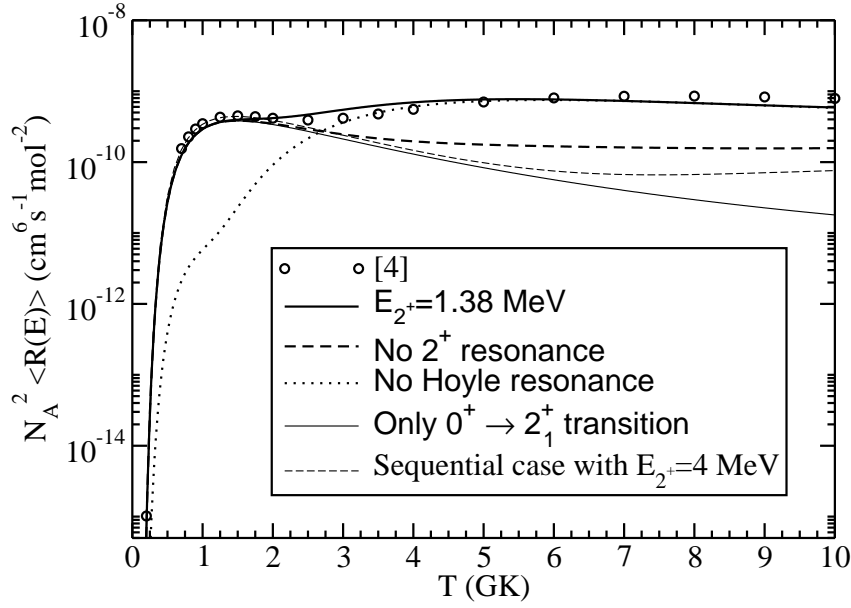


Fig. 5 Reaction rate after the full three-body calculation when the 2^+ resonance is placed at 1.38 MeV (thick solid line), when the resonance is removed from the calculation (thick dashed line), when the full contribution from the $2^+ \rightarrow 0_1^+$ transition is excluded (thin solid line), and when the Hoyle resonance is removed (dotted line). The thin solid curve is the calculation in the sequential case when the energy of the 2^+ resonance is 4.0 MeV. The open circles are the rate from [9].

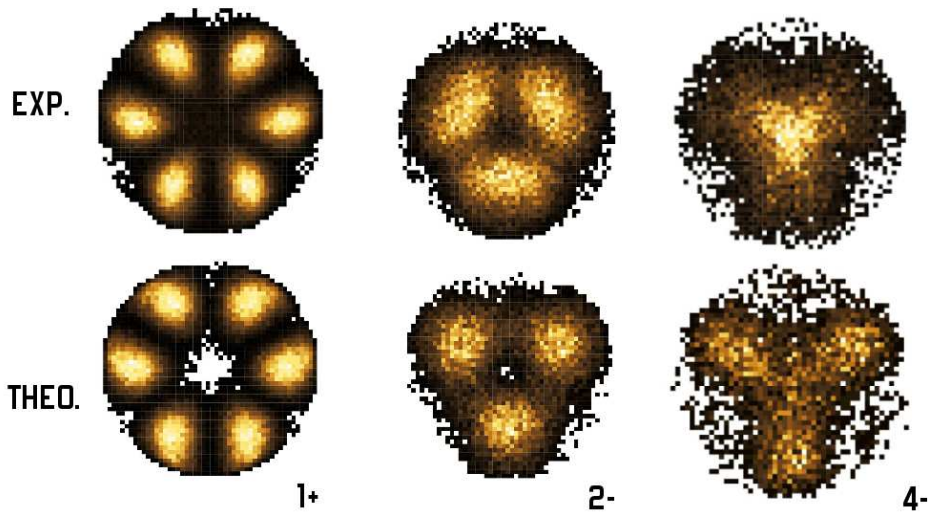


Fig. 6 The computed Dalitz plots for ^{12}C (1^+ , 2^- , 4^-)-resonances, compared to similar measured distributions. O.S. Kirsebom et al. Phys. Rev. C 81, 064313 (2010).

three-body energy. This gives rise to Dalitz plots which are two-dimensional probabilities as functions of two independent energies of the three-body system. For ^{12}C decaying into three α -particles the choice could be energies of two different α -particles for a given total resonance energy. We show computed examples in Fig. 6 for three resonances compared to experimental distributions. The similarities are striking where especially the zero points in the distributions are interesting. Some of these are unavoidable as inherent from the angular momentum, parity and symmetry of the wave function. Other zero points reflect the dynamical evolution and the decay mechanism and as such they are significant [11].

5 Recombination processes

The triple α process takes place when α -particles are present in a given volume. If a mixture of neutrons and α -particles is present two other recombination processes can also take place, that is creating ^6He and ^9Be consisting of one (two) α 's and two (one) neutrons. The relative creation rates are important for the continuation of the nuclear synthesis leading to different C-isotopes which in turn are the starting points for nuclear synthesis into heavier nuclei [8]. The density dependence of these rates is proportional to the number of particles involved in the given process where two (three) identical components should be counted twice (thrice). The temperature dependence is more complicated, depending for example on resonances, as seen in Figs. 4 and 5.

The density-temperature diagram is shown in Fig. 7 where $Y_\alpha = N_\alpha / (N_\alpha + N_n)$ is the relative fraction of α -particles. Very crudely, ^{12}C is predominantly created when the neutron density is low, correspondingly ^6He is predominantly created when the neutron density is high, and at intermediate densities the ^9Be creation dominates. The details of when and by how much the different processes contribute is not obvious. For example at low α -density and low temperature the ^9Be rate is larger than that of ^6He .

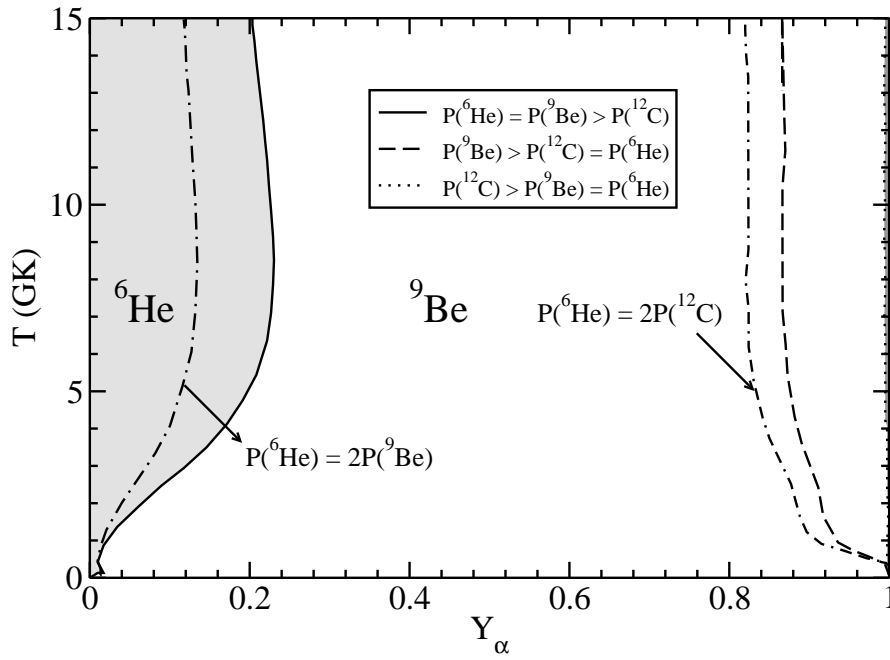


Fig. 7 The phase diagram for producing ${}^6\text{He}$, ${}^9\text{Be}$ and ${}^{12}\text{C}$ in the Y_α -temperature parameter space. The curves correspond to a constant ratio of production rates of two nuclei.

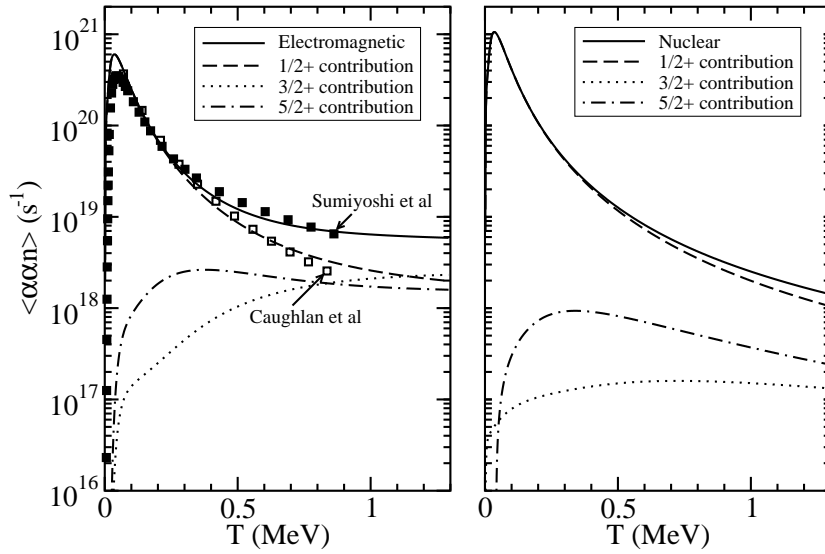


Fig. 8 The temperature averaged rates for ${}^9\text{Be}$ recombination from electromagnetic and nuclear processes. The nuclear rate is calculated for the neutron density of 10^{30} cm^{-3} . Sumiyoshi et al.: [6], Caughlan et al.: At. Data Nucl. Data Tables 40, 283 (1988).

This can be traced back to the low-lying $1/2^+$ resonance in ${}^9\text{Be}$. These results emerge from an interplay between recombination rates from individual three-body continuum states of different angular momentum and parity.

It is well known that radiative capture is much less efficient than capture where the photon is replaced by a particle of finite mass. In the environment, where neutrons and α 's are present with certain densities, there is always a finite probability of finding a fourth particle to substitute the photon and ensure energy and momentum conservation. This four-body recombination process is largest when the fourth particle is a neutron because it is neutral (not pushed away by the Coulomb repulsion) and its s -wave interaction with other neutrons is relatively large [12]. We compare nuclear and electromagnetic recombination rates in Fig. 8 for creating ${}^9\text{Be}$ as function of temperature for the continuum states of different angular momentum. They are remarkable similar but this is because we used a rather high neutron density to get contributions of the same order. The nuclear process has one additional neutron density as factor compared to the electromagnetic process. Thus at some density the processes must be of similar size as shown in Fig. 8.

6 Summary remarks

We use the hyperspherical adiabatic expansion method to investigate three-body resonance structures, decay mechanisms, and recombination rates for selected systems of light nuclei in stellar environments. We briefly discuss basic ingredients within the method, that is effective potentials, three-body resonance structure, partial decay widths, and momentum distributions of particles after the decay of the resonance. We also investigate recombination of three nuclear clusters into bound states of a light nuclei. We illustrate by examples of structure and decay properties of selected resonances in ${}^6\text{He}$, ${}^9\text{Be}$ and ${}^{12}\text{C}$. Specifically we show results for the influence of the 2^+ resonances in ${}^{12}\text{C}$ on the triple α -rate. We show the temperature and density dependence of the recombination rates from neutrons and α 's into ${}^6\text{He}$, ${}^9\text{Be}$ and ${}^{12}\text{C}$. We suggest an alternative route to bypass the $A = 5, 8$ gaps via nuclear four-body recombination processes. The possible comparison to measurements is very favorable.

References

1. E. Nielsen, D.V. Fedorov, A.S. Jensen and E. Garrido, The three-body problem with short-range interactions, *Phys. Rep.* **347**, 373 (2001).
2. A.S. Jensen, D.V. Fedorov, E. Garrido, Rearrangements in three-body decaying resonances, *J. Phys.* **G 37**, 064027 (2010).
3. R. Álvarez-Rodríguez, E. Garrido, A.S. Jensen, D.V. Fedorov, and H.O.U. Fynbo, Energy distributions from three-body decaying many-body resonances, *Phys.Rev.Lett.* **99**, 072503 (2007).
4. R. Álvarez-Rodríguez, H.O.U. Fynbo, A.S. Jensen, E. Garrido, Distinction between sequential and direct three-body decays, *Phys.Rev.Lett.* **100**, 192501 (2008).
5. E. Garrido, D.V. Fedorov, A.S. Jensen, Above threshold s -wave resonances illustrated by $1/2^+$ states in ${}^9\text{Be}$ ${}^9\text{B}$, *Phys.Lett.* **B 684**, 132 (2010).
6. K. Sumiyoshi, H. Utsunomiya, S. Goko, T. Kajino, Astrophysical reaction rate for $\alpha(\alpha n, \gamma){}^9\text{Be}$ by photodisintegration, *Nucl. Phys.* **A 709**, 467 (2002).
7. R. Álvarez-Rodríguez, A.S. Jensen, E. Garrido, D.V. Fedorov, Structure and three-body decay of ${}^9\text{Be}$ resonances, *Phys. Rev.* **C 82**, 034001 (2010).

-
8. R. de Diego, E. Garrido, D.V. Fedorov, A.S. Jensen, Relative production rates of ${}^6\text{He}$, ${}^9\text{Be}$, ${}^{12}\text{C}$ in astrophysical environments, *Europhys. Lett.*, **90**, 52001 (2010).
 9. C. Angulo et al., A compilation of charged-particle induced thermonuclear reaction rates, *Nucl. Phys.* **A 656**, 3 (1999).
 10. E. Garrido, D.V. Fedorov, H.O.U. Fynbo and A.S. Jensen, Energy distributions of charged particles from three-body decay, *Nucl. Phys.* **A 781**, 387 (2007).
 11. H.O.U. Fynbo, R. Álvarez-Rodríguez, A.S. Jensen, O.S. Kirsebom, D.V. Fedorov, E. Garrido, Three-body decays and *R*-matrix analyses, *Phys.Rev.* **C 79**, 054009 (2009).
 12. R. de Diego, E. Garrido, D.V. Fedorov and A.S. Jensen Alternative path for bridging the $A=5,8$ gap in neutron-rich nucleosynthesis scenarios, *J.Phys.* **G**, in press.